Oxidation of Metals, Vol. 45, Nos. 5/6, 1996

High-Temperature Corrosion of Ti and Ti–6Al–4V Alloy

H. L. Du,* P. K. Datta,* D. B. Lewis,† and J. S. Burnell-Gray*

Received August 4, 1993; revised June 26, 1995

Pure titanium and Ti–6Al–4V were exposed at 750°C in an $H_2/H_2O/H_2S$ ($P_{O_2} \sim 10^{-18}$ Pa and $P_{S_2} \sim 10^{-1}$ Pa), H_2/H_2O ($P_{O_2} \sim 10^{-18}$ Pa) and air environments for up to 240 hr. The corrosion kinetics, obtained by the discontinuous gravimetric method, showed that the sulfidation/oxidation kinetics were linear for Ti and linear-parabolic for Ti–6Al–4V in the $H_2/H_2O/H_2S$ environment. Both materials obeyed parabolic rate laws in the H_2/H_2O atmosphere after a transient period, and linear-parabolic rate laws in air. After exposure to the $H_2/H_2O/H_2S$ atmosphere, the titanium specimen displayed a double scale of TiO_2 with an intervening TiS_2 film between the double-layered scale of TiO_2 and the substrate. Ti–6Al–4V also contained a double layer of TiO_2 together with a stratum consisting of Al_2S_3, TiS_2 and vanadium sulfide at the junction of the inner TiO_2 layer and substrate. Some Al_2O_3 precipitated in the external portion of the outer TiO_2 layer. Following oxidation in the low-P_{O_2} atmosphere a double-layered oxide of TiO_2 scale formed on both Ti and Ti–6Al–4V. The scale on Ti–6Al–4V also contained an α-Al_2O_3 film situated between the outer and inner (TiO_2) layers. For both materials, multilayered-scale formation characterized air oxidation. In detail a multilayered oxide scale of TiO_2 formed on the air-oxidized Ti, while a multilayered oxide scale with alternating layers of Al_2O_3/TiO_2 developed on Ti–6Al–4V oxidized in air.

KEY WORDS: oxidation; sulfidation; oxides; sulfides; Ti; Ti–6Al–4V alloy.

INTRODUCTION

Environmental degradation of Ti and Ti alloys at elevated temperatures constitutes a major technological problem threatening to limit the exploitation

*Surface Engineering Research Group, University of Northumbria at Newcastle, United Kindom.

†Materials Research Institute, Sheffield Hallam University, United Kingdom.

0030-770X/96/0600-0507$09.50/0

of these materials. Ti is potentially a highly reactive metal capable of forming thermodynamically stable oxides, nitrides, carbides, and sulfides when exposed to oxygen, air, carbonaceous, and sulfur-containing gases. Of particular significance also is its ability to dissolve large quantities of gaseous species, a process accompanied by severe embrittlement. In general, at low temperatures (<400°C), the oxidation of Ti follows a logarithmic rate law, while at 400–600°C, a transient stage from logarithmic to parabolic or approximately cubic oxidation is observed. The oxidation rate of Ti in air and oxygen and other oxidizing media is typically parabolic at intermediate temperatures (600–700°C).[1–3] At higher temperatures breakaway-to-linear kinetics are observed after extended exposure, a process associated with the saturation of the metal, at the scale/metal interface, with oxygen and the formation of a porous scale.[4–7] Above 900°C, the linear rate of oxidation decreases with time.[1] The decreasing rate has been ascribed to the formation of a compact diffusion barrier layer within the scale caused by the sintering and grain growth of the oxide. The oxide formed on Ti oxidized below about 1000°C in near-atmospheric oxygen pressures consists generally of multiple layers of TiO_2 (rutile).[1]

A large number of studies have been published concerning the oxidation behavior of Ti-base alloys. The results derived from the oxidation of Ti–Al binary alloys are controversial. Menzies and Strafford[8] studied the oxidation behavior of Ti–5 wt.% Al in CO_2 at 1000°C and indicated that this alloy oxidized more rapidly than did pure titanium. However, Jenkins[9] showed that Ti–3 wt.% Al exposed to pure oxygen at temperatures between 750 and 900°C oxidized more slowly than did pure titanium, which was attributed to the formation of a protective scale of alumina due to the preferential oxidation of aluminum. Other workers[10–13] also found that addition of aluminum to titanium enhanced oxidation resistance since aluminum reduced the amount of oxygen dissolved in α-Ti; in detail it was reported[14] that the solubility of oxygen in titanium was reduced from 34 at.% to 0.3 at.% at 700°C. An α-Al_2O_3 layer was found near the external interface, and alumina was distributed in distinct sublayers of variable thickness. The number of alumina sublayers decreased with increasing temperature and above 950°C only an external alumina was identified. Other studies[14] revealed that alumina existed near the external interface either in the alpha or gamma form.

Welsch and Kahveci[15] observed the formation of mixed oxide scales on Ti–(26–49 at.%) Al alloys when oxidized in dry oxygen ($P_{O_2} \sim 10^5$ Pa) between 600 and 1100°C. These scales contained increasing amounts of Al_2O_3, interspersed heterogeneously with TiO_2 and included a predominantly Al_2O_3-rich sublayer with increasing aluminum contents. γ-TiAl also formed alumina scales below ~1000°C in oxygen but developed mixed titanium and aluminum oxide scales at higher temperatures.[16] The formation of

a protective Al_2O_3 scale on Al_3Ti in pure oxygen in a temperature range 800–1000°C has also been reported.[17]

Some efforts have been made to promote the formation of an external alumina layer by the addition of ternary elements. It is believed that the ability of Ti–Al alloys to develop a protective Al_2O_3 layer should be increased by (1) increasing the diffusion of Al; (2) reducing the solubility and diffusion of oxygen; and (3) decreasing or eliminating the transient periods. Accordingly, the positive effects of Nb,[18,19] Ta, Ag,[20] W,[14,21] and Re, Mo, and Cr[21] on the oxidation behavior of Ti–Al binary alloys have been reported. Hf had only a marginal effect whilst Ga proved to be detrimental.[18] The addition of 1.4 wt.% V was observed to prevent the formation of an Al_2O_3 barrier at the interface of the inner and outer layers of TiO_2 and the oxidation rate increased.[19] Wallance *et al.*[22] studied the oxidation behavior of Ti–25Al–10Nb–3V–1Mo (at.%) in air over the temperature range of 650–1000°C and showed that additions of V and Mo did not substantially change the oxidation behavior of this alloy compared to that observed for Ti–24Al–10Nb, but its overall oxidation rate was much lower than that for Ti_3Al.

The kinetics and mechanisms of the oxidation/sulfidation reaction for Ti and Ti-base alloys have, however, not been studied extensively. In particular there is a lack of data concerning their behavior in environments comprising low-oxygen/high-sulfur partial pressures.

In this work, the sulfidation/oxidation behavior of titanium and Ti–6Al–4V was studied at 750°C in an atmosphere comprising $P_{O_2} \sim 10^{-18}$ Pa and $P_{S_2} \sim 10^{-1}$ Pa, which is known to be extremely aggressive even for the most sophisticated high-temperature alloys. Also, the oxidation behavior of Ti and Ti–6Al–4V in air and low P_{O_2} ($\sim 10^{-18}$ Pa) at 750°C was investigated.

EXPERIMENTAL PROCEDURES

The materials used in this program included commercially pure titanium and Ti–6Al–4V alloy (IMI Titanium 318) supplied by IMI Titanium Ltd. in rod form. These rods were machined to produce coupons of diameter 12.5 mm and 1.5 mm thick for use in this program. A 1-mm-diameter hole was drilled at the edge of each sample to facilitate suspension within the working tube. All coupons were polished using SiC paper up to 1200 grit followed by ultrasonic cleaning and degreasing in acetone for 30 min.

The prepared specimens were exposed in $H_2/H_2O/H_2S$ ($P_{O_2} \sim 10^{-18}$ Pa and $P_{S_2} \sim 10^{-1}$ Pa), H_2/H_2O ($P_{O_2} \sim 10^{-18}$ Pa) and circulating air environments at 750°C. The corrosion kinetics followed by the Ti and Ti–6Al–4V were recorded using a discontinuous gravimetric method. High-purity hydrogen and premixed 90% H_2/10% H_2S mixture, which was chosen to yield a P_{S_2} value of 10^{-1} Pa at the reaction temperature of 750°C, were

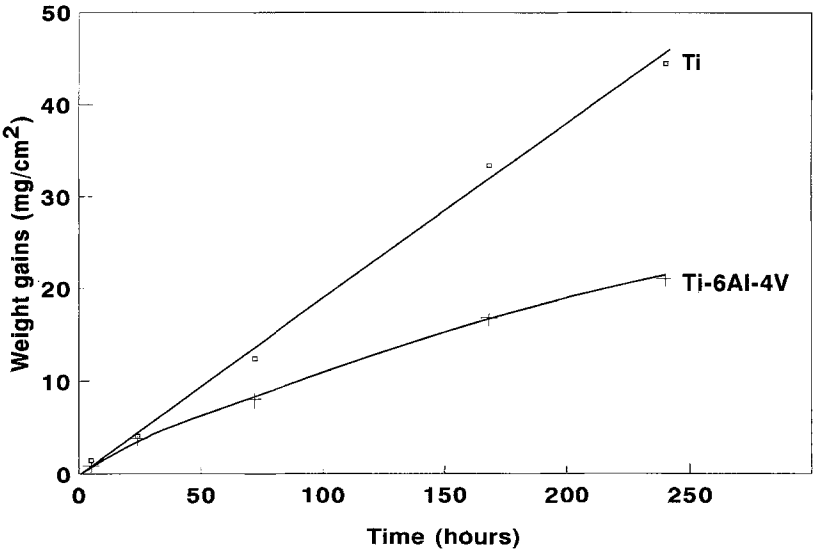

Fig. 1. Weight gains vs. exposure time for Ti and Ti–6Al–4V exposed to an $H_2/H_2O/H_2S$ environment at 750°C.

passed through two gas bubblers, containing deionized water, held in a water bath maintained at a constant temperature (23°C) in order to achieve an oxygen potential of 10^{-18} Pa at 750°C. Details of the experimental rig have been reported elsewhere.[23–25] In order to investigate the diffusion direction of anions and cations, a marker study was carried out using E8300 conductive platinum-based firing enamel which contained 84 wt.% Pt. The Pt paint was brushed on the samples following drying in open air at 100°C for 30 min. The corrosion products generated on the specimens were characterized by means of scanning electron microscopy (SEM), energy-dispersive analysis by X-ray (EDX) and X-ray diffraction (XRD).

EXPERIMENTAL RESULTS

Kinetics

Figures 1–3 show the corrosion kinetics of Ti and Ti–6Al–4V at 750°C in $H_2/H_2O/H_2S$, H_2/H_2O, and air environments, respectively. It is apparent that in the $H_2/H_2O/H_2S$ environment the corrosion behavior of pure Ti followed a linear rate law with a linear rate constant of 5.7×10^{-8} g/cm^2/s, while that of Ti–6Al–4V obeyed quasi-parabolic kinetics with the corrosion rate decreasing with exposure time. Ti–6Al–4V displayed better sulfidation/oxidation resistance than did pure titanium. The oxidation kinetics of Ti

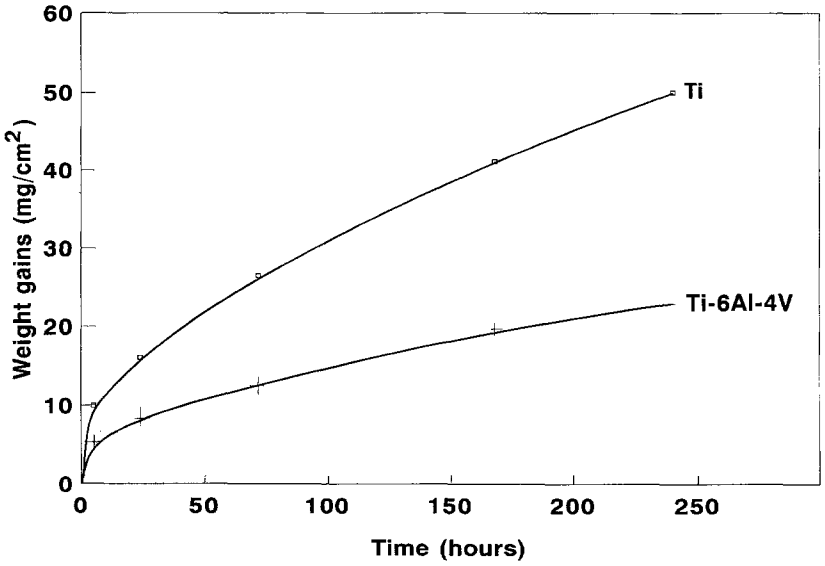

Fig. 2. Weight gains vs. exposure time for Ti and Ti–6Al–4V oxidized in an H_2/H_2O environment at 750°C.

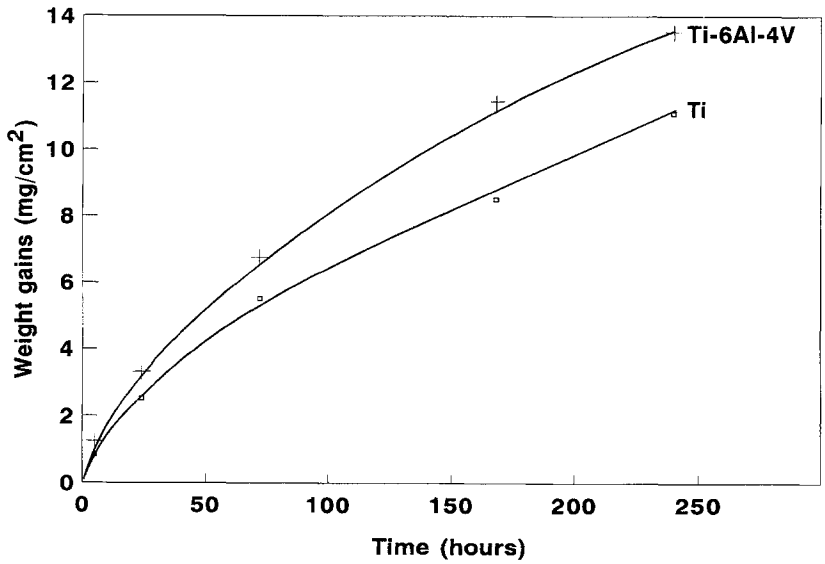

Fig. 3. Weights gains vs. exposure time for Ti and Ti–6Al–4V oxidized in air at 750°C.

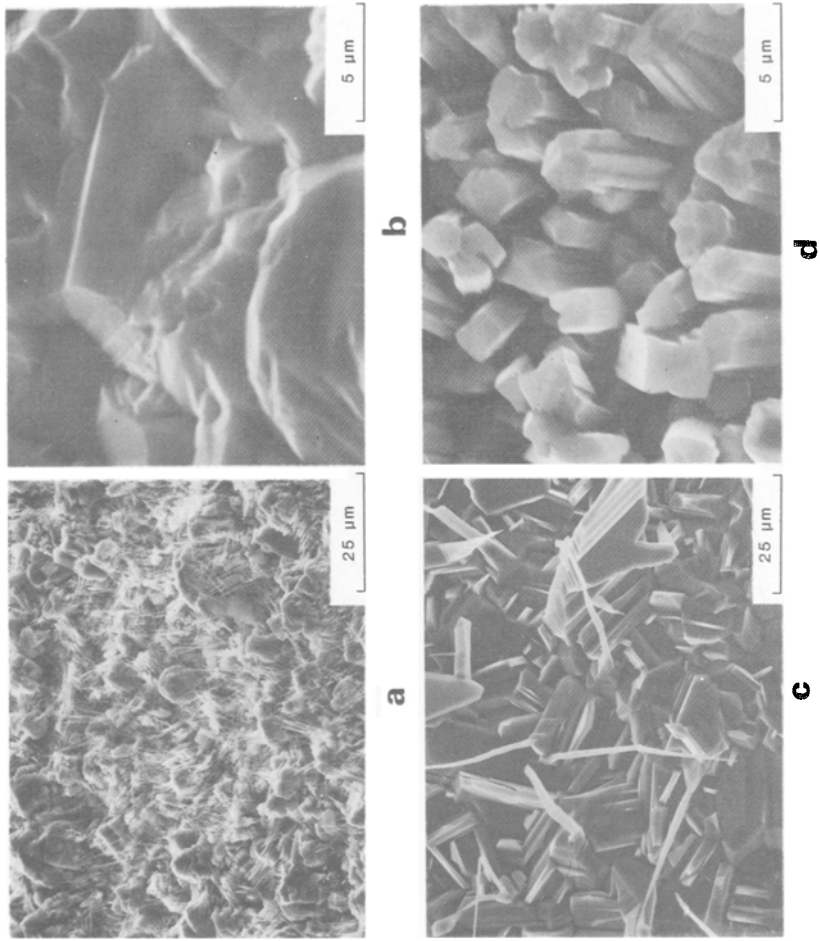

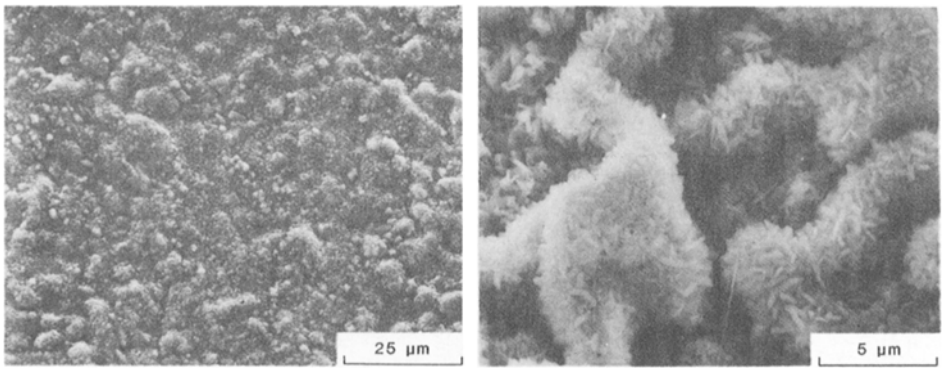

Fig. 4. Scanning electron micrographs showing typical surface morphologies of Ti and Ti–6Al–4V after exposure for 72 hr at 750°C: (a) Ti and (b) Ti–6Al–4V in $H_2/H_2O/H_2S$; (c) Ti and (d) Ti–6Al–4V in H_2/H_2O; (e) Ti and (f) Ti–6Al–4V in air.

and Ti–6Al–4V in the low-P_{O_2} atmosphere (Fig. 2) obeyed strictly the parabolic rate law after an early transient period (~5 hr), giving *Kp* values of 2.9×10^{-9} g^2/cm^4/s for Ti and 6.5×10^{-10} g^2/cm^4/s for Ti–6Al–4V. The oxidation behavior of Ti and Ti–6Al–4V in air (Fig. 3) followed linear-parabolic kinetics. It is also noticeable that although the oxidation resistance of Ti–6Al–4V in the low-P_{O_2} atmosphere was superior to that of pure titanium, the additions of Al and V alloying elements were detrimental to the oxidation resistance of Ti in air.

To summarize, the corrosion rate of Ti and Ti–6Al–4V was fastest in the H_2/H_2O environment, least in air and followed an intermediate rate in the $H_2/H_2O/H_2S$ atmosphere; i.e.,

$$\text{high } P_{O_2}\text{ (air)} > \text{low } P_{O_2}/\text{high } P_{S_2} > \text{low } P_{O_2}$$

Corrosion Products

The scale morphologies developed on Ti and Ti–6Al–4V at 750°C in these environments showed remarkable differences. Figure 4 reveals the surface morphologies of Ti and Ti–6Al–4V after 72 hr corrosion in the three atmospheres. In the $H_2/H_2O/H_2S$ atmosphere used here (Figs 4a, b), a dense and compact scale formed on Ti, while a relatively rough and compact scale developed on Ti–6Al–4V. Only TiO_2 was identified by XRD on pure titanium and TiO_2 and Al_2O_3 on Ti–6Al–4V. In the H_2/H_2O atmosphere, TiO_2 and Al_2O_3 were detected by XRD on Ti–6Al–4V at the early stages of exposure (e.g. 5 hr). However, after prolonged exposure, XRD detected only (dendritic) TiO_2, which implied that the Al_2O_3 phase became buried by the rutile scale. The oxide scale formed on Ti consisted of TiO_2. Scanning electron micrographs showing the morphologies of Ti and Ti–6Al–4V exposed to the H_2/H_2O atmosphere for 72 hr are included in Figs. 4c, d. The scale on Ti–6Al–4V is characterized by a dendritic morphology which persisted even up to the end of the experiment (240 hr). Under the air oxidation condition (Figs 4e, f), convoluted TiO_2 scales formed on the pure Ti while flower-like products, identified by XRD as Al_2O_3, developed on Ti–6Al–4V. It is important to point out that the Al_2O_3 phase was still detected on Ti–6Al–4V after increasing exposure time, and the morphological features did not significantly change with exposure period.

The cross-sectional micrographs of the corrosion products developed on pure titanium and Ti–6Al–4V exposed to the $H_2/H_2O/H_2S$ environment, as illustrated in Figs. 5 and 6, respectively, reveal that the scales consisted basically of two sublayers. For pure Ti, the XRD results showed that both the outer layer and the inner layer comprised TiO_2 (rutile), and no compositional nor phase differences were evident between these two layers. It has been demonstrated by a marker study that the outer layer formed by the

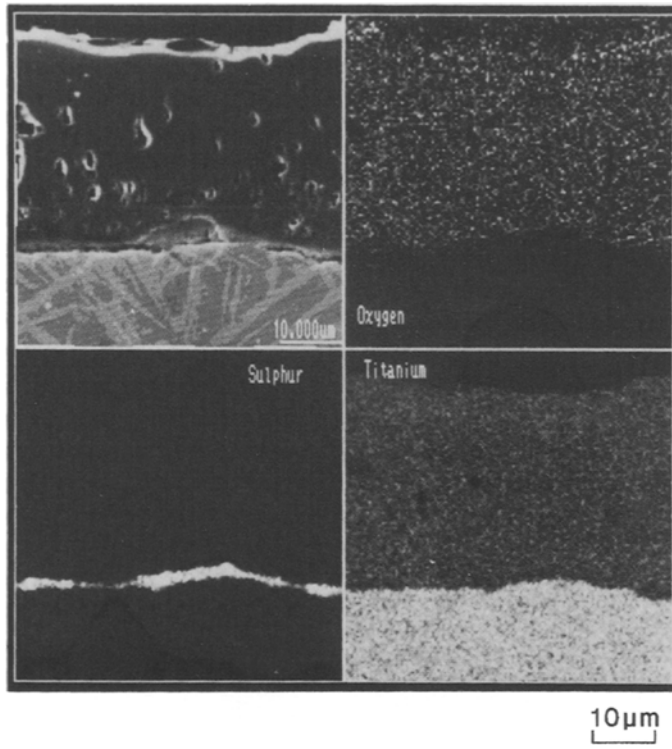

Fig. 5. Electron image and X-ray maps showing typical compositional profiles through the scale on Ti after 72 hr exposure to an $H_2/H_2O/H_2S$ environment at 750°C.

outward diffusion of titanium, while the inner layer was produced by the inward diffusion of oxygen. As shown in Fig. 7, Pt was segregated at the outer/inner layer interface. In addition, for pure titanium a TiS_2 layer was found to exist beneath the rutile scale, and a great deal of titanium hydride, identified by XRD as TiH_2, was present in the substrate as indicated in Fig. 5. In this environment at elevated temperature, hydrogen was readily absorbed by the substrate and subsequently precipitated to give a needle-like structure of TiH_2. In the case of Ti–6Al–4V, Al-enrichment was evident in the external portion of the outer layer; i.e., a mixture of Al_2O_3 and TiO_2 was present. However, a pure TiO_2 layer formed beneath this mixed layer. A mixture of sulfides of Al, Ti, and V was detected by EDX between the TiO_2 oxide scale and the substrate. The presence of Al_2S_3 and TiS_2 was identified by XRD. However, XRD failed to reveal any presence of the vanadium sulfide, perhaps because of its low concentration.

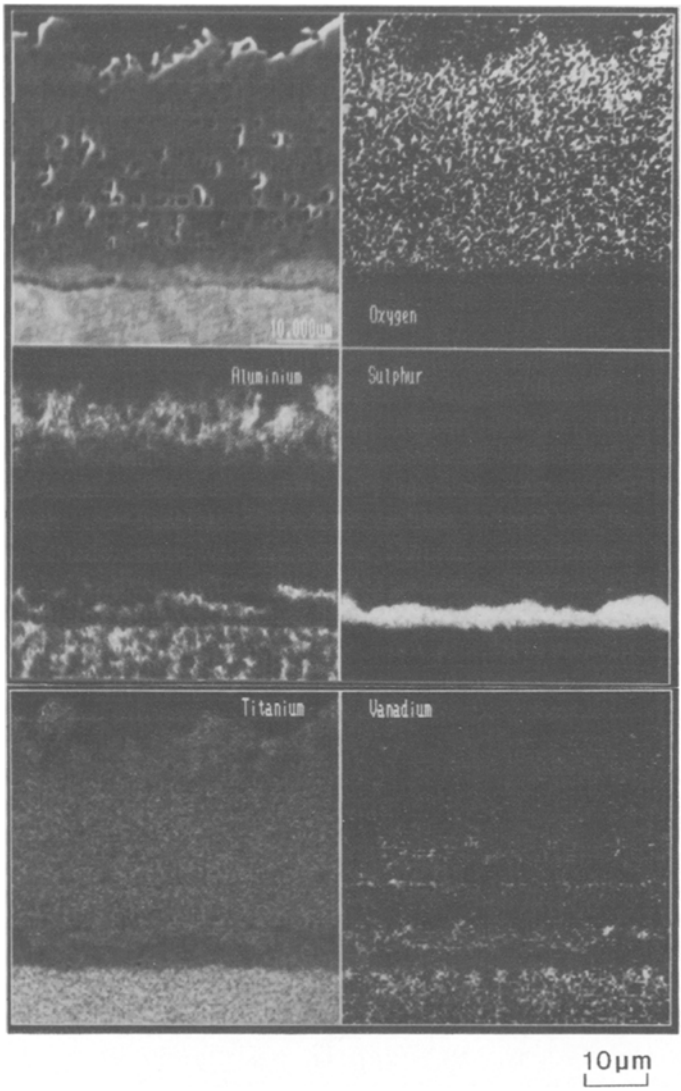

Fig. 6. Electron image and X-ray maps showing typical compositional profiles through the scale on Ti–6Al–4V after 72 hr exposure to an $H_2/H_2O/H_2S$ environment at 750°C.

Significantly, vanadium oxide was found at the interface of the outer layer and inner layer. No titanium hydride was evident in this alloy even after 240 hr exposure.

Figure 8 depicts the EDX results from a cross section through the surface of pure titanium after 240 hr exposure in the low-P_{O_2} atmosphere.

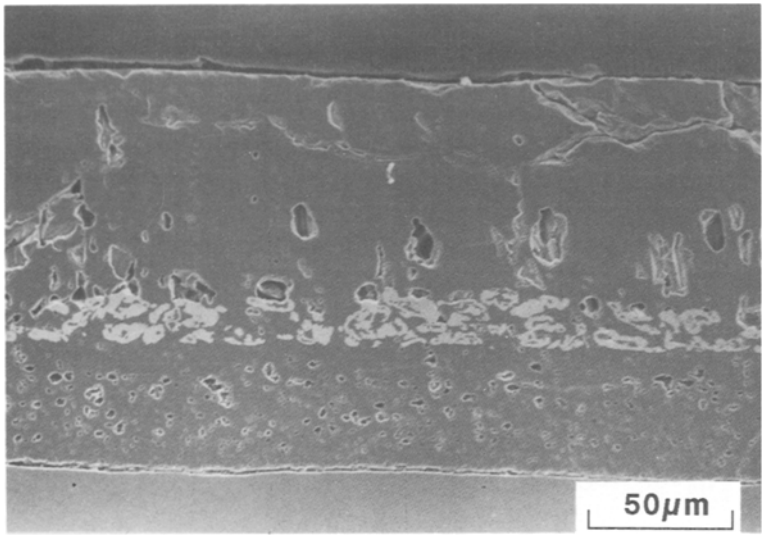

a

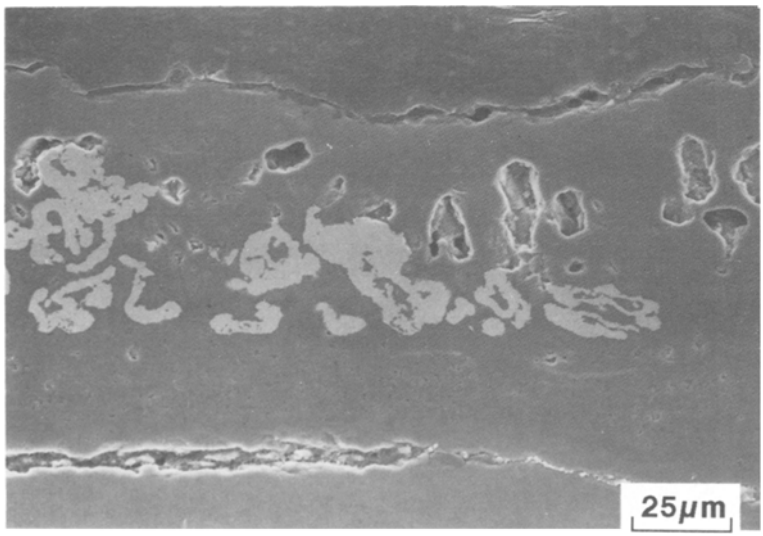

b

Fig. 7. Scanning electron micrographs showing cross-sectional morphologies of Ti and Ti–6Al–4V after exposure for 168 hr at 750°C: (a) Ti and (b) Ti–6Al–4V.

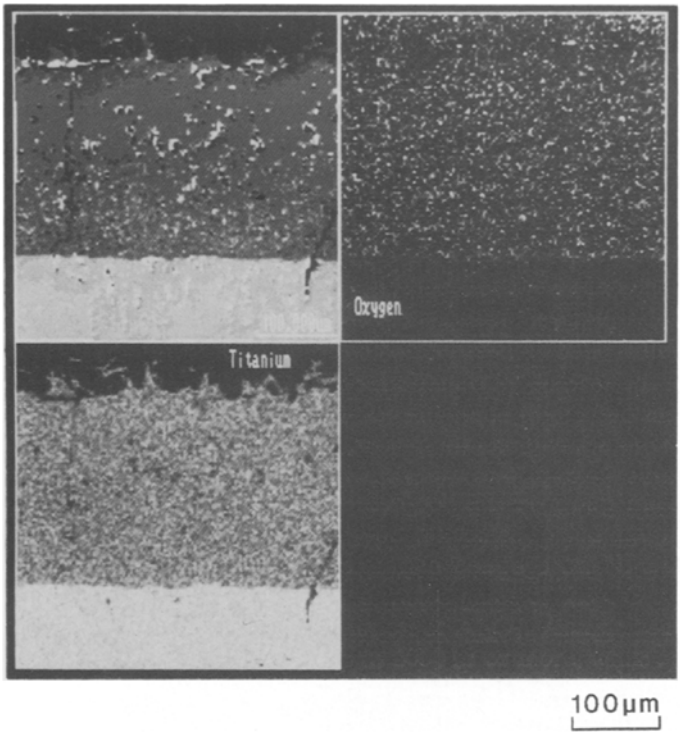

Fig. 8. Electron image and X-ray maps showing typical compositional profiles through the scale on Ti after 240 hr exposure to an H_2/H_2O environment at 750°C.

Two subscale layers comprised the oxide scale (TiO_2); in the outer layer, a few relatively large voids were present, while the inner layer was observed to contain numerous small voids. The entire oxide scale was characterized by the presence of some transverse cracks, which penetrated the substrate, across the whole oxide scale. In addition, a large amount of TiH_2 was found in the substrate after each exposure period. For Ti–6Al–4V, Al_2O_3 was observed on top of the TiO_2 layer after 5 hr exposure. However with increasing exposure time, a dendritic TiO_2 outer layer was observed, and a continuous layer of Al_2O_3 formed between the outer and inner layers of TiO_2, as shown in Fig. 9. Evidently, vanadium oxide developed beneath the Al_2O_3 layer, but XRD failed to identify the exact vanadium oxide phase due perhaps to the very small quantities involved.

A multilayered TiO_2 scale was observed on the cross section of pure titanium after exposure in air at 750°C, as shown in Fig. 10. The TiO_2 scale

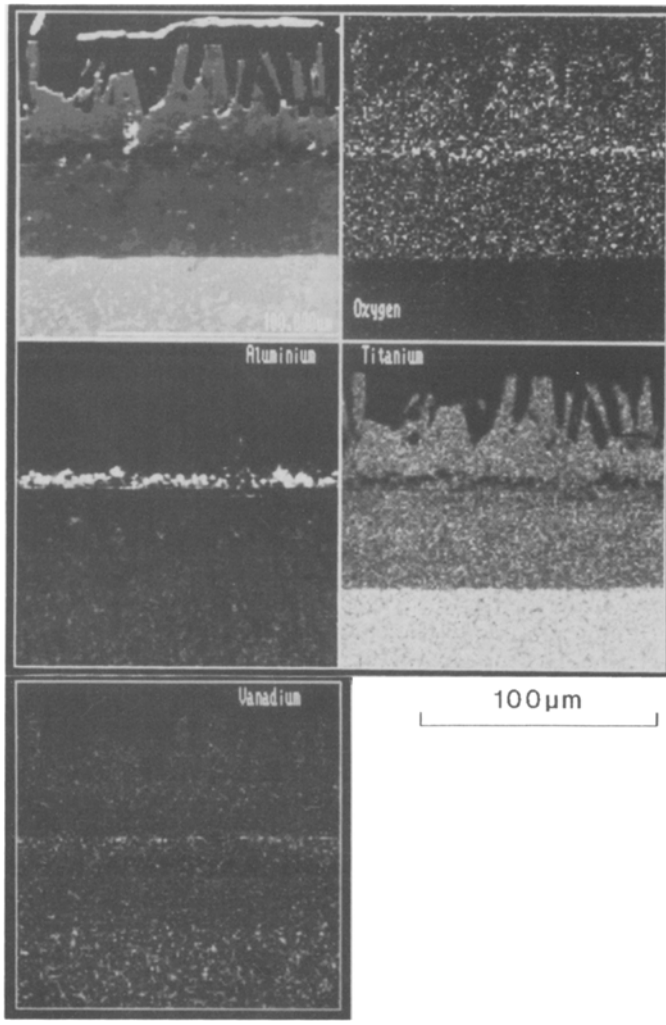

Fig. 9. Electron image and X-ray maps showing typical compositional profiles through the scale on Ti–6Al–4V after 240 hr exposure to an H_2/H_2O environment at 750°C.

was marked by a series of cracks oriented parallel to the sample surface. The external portion of the scale comprised numerous voids, whereas smaller and fewer voids characterized the inner portion of the scale. Figure 11 shows X-ray maps for Ti–6Al–4V after 240 hr air oxidation. It is apparent from the images that a multilayered scale developed in which Al_2O_3 remained

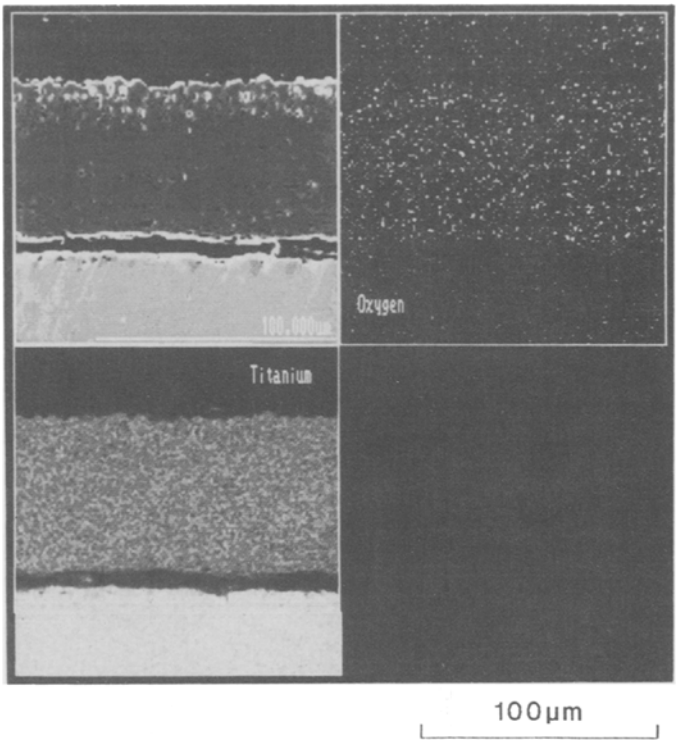

Fig. 10. Electron image and X-ray maps showing typical compositional profiles through the scale on Ti after 240 hr air oxidation at 750°C.

sandwiched between the TiO_2 layers. A more detailed study using a range of different exposure periods and even different reaction temperatures[26] revealed that the external gas–oxide interface was always occupied by an Al_2O_3 layer. The number of the sandwiched Al_2O_3 layers increased with increasing exposure time. Cracks occurring at the interfaces between Al_2O_3 and TiO_2 layers indicated poor adhesion. Both Ti and Ti–6Al–4V showed the formation of large cracks between the oxide scale and substrate.

It should be pointed out that the over-enhanced vanadium signal seen in the outer layer in the vanadium-distribution maps may have been due to the $Ti_{K_\beta}/V_{K_\alpha}$ overlap in the energy dispersive X-ray spectrum. The ratio of $Ti_{K_\alpha}/Ti_{K_\beta}$ is known to be approximately 8.5:1 at 15 kV which was employed in the examination, then since the Ti_{K_α} is not overlapped by the other elements this is used as a measure of the Ti_{K_β} contribution to

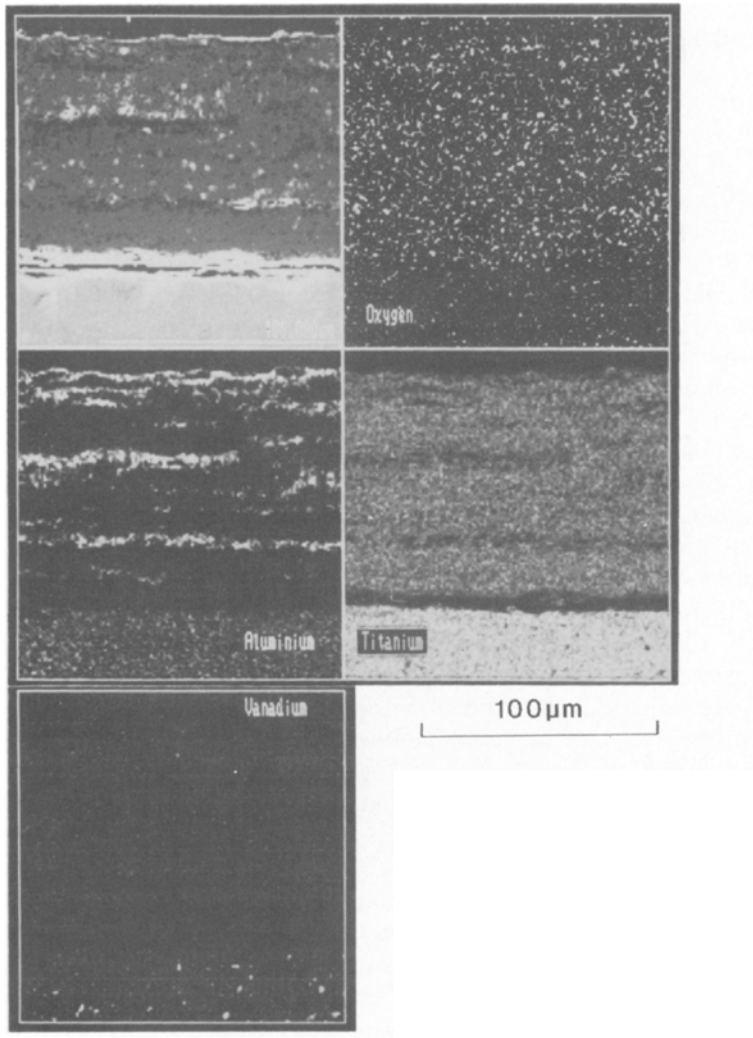

Fig. 11. Electron image and X-ray maps showing typical compositional profiles through the scale on Ti–6Al–4V after 240 hr air oxidation at 750°C.

the map, i.e.,

$$Ti_{K_\beta} = Ti_{K_\alpha}/8.5$$

The Ti_{K_β} contribution is thus removed from the image leaving only the

V_{K_α}. It is possible, however, that this stripping routine was not complete, resulting in an apparent vanadium signal.

DISCUSSION

For pure titanium exposed at 750°C to the $H_2/H_2O/H_2S$ environment used, the corrosion products comprised two TiO_2 layers beneath which a TiS_2 film was identified. Similar exposure of Ti–6Al–4V to the $H_2/H_2O/H_2S$ environment at 750°C promoted the formation of a double TiO_2 scale beneath which a layer of primarily Al_2S_3 existed. α-Al_2O_3 also precipitated in the external portion of the outer layer of TiO_2. The outer layer of TiO_2 formed on both Ti and Ti–6Al–4V developed by the outward diffusion of titanium. The formation of the inner layers can occur by two possible mechanisms: (i) by ingress of oxygen species, molecular or anionic, directly from the gaseous phase,[27–29] or (ii) by ingress of oxygen species derived from the dissociation of the outer layer.[30–32] In the present case, the dissociative mechanism can be ruled out because both the outer layer and the inner layer consisted of the same phase (TiO_2). Therefore the conclusion is that the inner layer of TiO_2 was formed by the ingress of oxygen species from the bulk environment; i.e., some oxygen species diffused toward the substrate and reacted with the titanium species from the substrate. However, it is suggested that the outward flux of titanium was greater than the inward flux of oxygen species since the growth of the outer layer depended on the outward migration of the titanium and furthermore the outer layer was much thicker than the inner layer, as shown in Figs. 5 to 7.

The values of P_{S_2}, P_{O_2}, a_{Al}, and a_{Ti} would each influence the formation of the corrosion products. Considering the experimental results, it is assumed that a double-layered TiO_2 scale formed at the initial stages of exposure, beneath which a TiS_2 layer on Ti and a primarily Al_2S_3 layer on Ti–6Al–4V developed. Then the gradients of P_{O_2}, P_{S_2}, a_{Al}, and a_{Ti} were established across the oxide–sulfide scale. Obviously, P_{O_2} and P_{S_2} decreased, while a_{Al} and a_{Ti} increased toward the substrate. Thus, the reactions at the oxide–sulfide interface for both Ti and Ti–6Al–4V can be defined by

$$Ti(s) + O_2(g) = TiO_2(s) \tag{1}$$

and

$$Ti(s) + S_2(g) = TiS_2(s) \tag{2}$$

for pure titanium and

$$2Al(l) + (3/2)S_2(g) = Al_2S_3(s) \tag{3}$$

for Ti–6Al–4V.

At the sulfide–substrate interface, reactions (2) and (3) also will occur. For all three reactions, assuming unit activity for the reaction products, TiO_2, TiS_2, and Al_2S_3 equilibrium constants can be defined as

$$K_1 = K_{TiO_2} = a_{Ti}^{-1} \cdot P_{O_2}^{-1} \tag{4}$$

$$K_2 = K_{TiS_2} = a_{Ti}^{-1} \cdot P_{S_2}^{-1} \tag{5}$$

and

$$K_3 = K_{Al_2S_3} = a_{Al}^{-2} \cdot P_{S_2}^{-3/2} \tag{6}$$

At the TiO_2/Al_2S_3 interface for the Ti–6Al–4V alloy, if insufficient sulfur species arrive from the atmosphere and a limited amount of aluminum is transported from the substrate, then the position of the equilibrium in reaction (3) will shift to the left with Al_2S_3 being decomposed at the TiO_2–Al_2S_3 interface. The aluminum species released will diffuse outwards and the freed sulfur species will migrate inward.

Considering the formation of Al_2O_3,

$$2Al(l) + (3/2)O_2(g) = Al_2O_3(s) \tag{7}$$

provided the activity of Al_2O_3 is one, the equilibrium constant for reaction (7) will follow:

$$K_7 = K_{Al_2O_3} = a_{Al}^{-2} \cdot P_{O_2}^{-3/2} \tag{8}$$

At a certain point of the external part of the outer layer of TiO_2, the oxygen partial pressure will be high enough to make the equilibrium in reaction (7) shift to the right and as a result Al_2O_3 will precipitate, as shown in Fig. 6. At the same time the freed sulfur species will migrate inward through the Al_2S_3 layer to the sulfide–substrate interface where high aluminum activity in the substrate will ensure the formation of Al_2S_3. With progressive corrosion, the relative activities of Ti, Al, and V might be altered and Ti and V sulfides might also be formed, as revealed in Fig. 6. It is apparent that the dissociation of Al_2S_3 will simply move the oxide–sulfide interface inward but not increase the thickness of the sulfide layer. Therefore, the sulfide layer must be thickened by the ingress of sulfur species from the bulk environment. It is expected that a similar reaction process will occur for pure titanium giving TiS_2, although it has not been possible to identify any TiO_2 precipitate produced by the reaction of oxygen species and titanium released from the dissociation of TiS_2 in the external portion of the outer layer of the TiO_2.

Exposure of Ti–6Al–4V to the H_2/H_2O atmosphere ($P_{O_2} \sim 10^{-18}$ Pa) caused a TiO_2 layer to develop, this oxide being thermodynamically favored to form due to the high titanium activity in the alloy. Subsequently, aluminum diffused outward, and an α-Al_2O_3 layer formed at the external interface

of gas–oxide. This double-layered oxide scale was observed at the early stages of oxidation (e.g., 5 hr). Once the double-layered-oxide scale was established, reactions (1) and (7) were possible at the Al_2O_3/TiO_2 interface. At the TiO_2 layer–substrate interface, reaction (1) also occurred. Assuming the activities of the reaction products, $a_{Al_2O_3}$ and a_{TiO_2}, equal to one, then the equilibrium constants for reactions (1) and (7) can be expressed by Eqs. (4) and (8). Owing to the formation of an Al_2O_3 layer at the external interface of gas–oxide, the P_{O_2} value beneath the Al_2O_3 layer will be reduced. If insufficient titanium diffuses to this interface, the equilibrium in reaction (1) will move to the left. If it is assumed that the values of P_{O_2} at the Al_2O_3–TiO_2 interface are either 10^{-18} Pa (highest possible value), which is equal to that in the bulk atmosphere, or 10^{-41} Pa (lowest possible value) which is equivalent to the dissociation partial pressure of Al_2O_3, then the minimum aluminum activities for the formation of Al_2O_3 should be 6.6×10^{-18} or 1, and likewise the minimum titanium activities required to form TiO_2 should be 3.7×10^{-15} or 3×10^{8}. In both extremes, it is obvious that the minimum aluminum activities for the formation of Al_2O_3 are much smaller than the minimum titanium activities for the formation of TiO_2. At the Al_2O_3–TiO_2 interface, the actual values of oxygen partial pressures should be more than the dissociation partial pressure of Al_2O_3 ($\sim 10^{-41}$ Pa) but less than the P_{O_2} in the bulk environment ($\sim 10^{-18}$ Pa). Consequently, the condition at this interface is more favorable for the formation of Al_2O_3, while TiO_2 would decompose. The released titanium then migrates outward through the Al_2O_3 layer and arrives at the external gas–oxide interface where the relatively high oxygen partial pressure ($\sim 10^{-18}$ Pa) in the bulk environment promotes the formation of a TiO_2 layer, as revealed in Fig. 9. The freed oxygen species from the dissociation of TiO_2 are partially consumed by the formation of the Al_2O_3 layer and partially transported to the TiO_2–substrate interface where high titanium activity in the substrate makes it possible to form TiO_2. It should be pointed out that the formation of TiO_2 at the TiO_2–substrate interface is further enhanced by the ingress of the oxygen species from the bulk environment.

The mechanisms responsible for the oxidation of Ti–6Al–4V in air between 650 and 850°C have been described in another paper.[26] It was observed that a multilayered scale developed on Ti–6Al–4V oxidized in air. TiO_2 and Al_2O_3 grew alternatively and Al_2O_3 remained sandwiched between the TiO_2 layers. The number of the sandwiched Al_2O_3 layers increased with increasing temperature and exposure time. Cracks occuring at the interfaces between the Al_2O_3 and TiO_2 layers indicated poor adhesion. The formation of large cracks between the oxide scale and substrate was observed. Here an alternating multilayered Al_2O_3–TiO_2 scale formed on Ti–6Al–4V which provided more constraint to plastic flow than did the oxide formed on pure

titanium and hence was more likely to form cracks between the oxide scale and alloy substrate. In general, the cracks caused detachment of the oxide from the substrate. Thus, the cracking tendency of the multilayered Al_2O_3–TiO_2 scale reduced the oxidation resistance of the alloy by rendering the Al_2O_3 less protective. In contrast, in the H_2/H_2O atmosphere, the Al_2O_3 layer, situated at the interface of the outer layer and inner layers, acted as a diffusion barrier slowing down the outward migration of titanium and inward diffusion of the oxygen species and thereby promoted superior oxidation resistance compared to pure titanium. In the sulfur–oxygen environment, the formation of Al_2O_3 in the external portion of the outer layer, to some extent, inhibited the diffusion of the reactants. Furthermore, the gradual development of vanadium sulfide significantly influenced the corrosion resistance. The positive effect of vanadium on the sulfidation behavior has been widely reported.[24,25,33,34]

It is also noted that the sulfidation–oxidation rates for titanium and Ti–6Al–4V in the $H_2/H_2O/H_2S$ environment were slower than the corresponding oxidation rates in H_2/H_2O, despite the oxygen partial pressures being identical ($P_{O_2} \sim 10^{-18}$ Pa). The presence of H_2S in the atmosphere probably poisoned the TiO_2 nucleation sites and reduced the number of TiO_2 nuclei at the early stages of corrosion, and as a result a relatively low corrosion rate was observed. On the other hand, the low parabolic sulfidation constant of Ti ($\sim 10^{-12}$ g^2/cm^4/s)[33] did not make a significant contribution to the total corrosion rate. Sulfur in the form of H_2S at low concentrations (<100 ppm) is commonly added to carburizing environments[35] to reduce the carburization rate. Grabke *et al.*[36] found that the rate of carburization in H_2/CH_4 decreased with increasing sulfur activity (H_2S content) of the gas mixture below a critical sulfur activity at which sulfidation became the major corrosion problem. It is thought that H_2S may have a similar effect in the H_2/H_2O atmospheres. These observations support the conclusion concerning the lower sulfidation–oxidation rate of Ti and Ti–6Al–4V in $H_2/H_2O/H_2S$ than in H_2/H_2O.

CONCLUSIONS

1. Oxidation of Ti and Ti–6Al–4V in air followed linear-parabolic kinetics and the Ti–6Al–4V oxidized faster than pure titanium.

2. Oxidation of Ti and Ti–6Al–4V in the H_2/H_2O ($P_{O_2} \sim 10^{-18}$ Pa) atmosphere followed a parabolic rate law after a transient period and Ti–6Al–4V oxidized slower than pure titanium.

3. In the $H_2/H_2O/H_2S$ ($P_{O_2} \sim 10^{-18}$ Pa and $P_{S_2} \sim 10^{-1}$ Pa) environment Ti followed a linear rate law, while Ti–6Al–4V obeyed a linear-parabolic rate law. Additions of Al and V enhanced the corrosion resistance.

4. For each exposure period (up to 240 hr) used in this study, the fastest corrosion rate was observed in the H_2/H_2O environment and the slowest corrosion rate was recorded in air. The corrosion rate of Ti and Ti–6Al–4V can be ranked as: air $< H_2/H_2O/H_2S < H_2/H_2O$.

5. A multilayered-oxide scale of TiO_2 typified Ti oxidized in air, whereas a multilayered-oxide scale with alternating layers of Al_2O_3/TiO_2 characterized Ti–6Al–4V oxidized in air.

6. A double-layered-oxide (TiO_2) scale was identified on oxidized Ti in the low-P_{O_2} atmosphere, and an α-Al_2O_3 layer was also detected between the outer layer and inner layer of TiO_2 for Ti–6Al–4V.

7. In the $H_2/H_2O/H_2S$ atmosphere the corrosion products generated on pure titanium were characterized by a double-layered-oxide scale of TiO_2 beneath which a TiS_2 layer was observed. For Ti–6Al–4V, α-Al_2O_3 had precipitated in the external portion of the outer TiO_2 layer, and a layer of Al_2S_3, TiS_2, and vanadium sulfide was found underlying the inner TiO_2 layer.

8. On exposure of Ti and Ti–6Al–4V to the $H_2/H_2O/H_2S$ atmosphere H_2S poisoned the TiO_2 nucleation sites. This, together with the low-sulfidation parabolic rate constant for Ti, reduced the corrosion rate at the early stages of exposure. However, H_2S accelerated the corrosion rate after prolonged exposure.

ACKNOWLEDGMENTS

Grateful acknowledgment is given for the financial funding of Dr. H. L. Du, as a research fellow, at the University of Northumbria at Newcastle, and Dr. D. B. Lewis, as senior research fellow, at Sheffield Hallam University, by the Science and Engineering Research Council's Rolling Grant in Surface Engineering.

REFERENCES

1. P. Kofstad, *High Temperature Corrosion* (Elsevier Applied Science, London, 1988).
2. J. E. Lopes Gomes and A. M. Huntz, *Oxid. Met.* **14**, 249 (1980).
3. J. Unnam, R. N. Shenoy, and R. K. Clark, *Oxid Met.* **26**, 231 (1986).
4. I. A. Menzies and K. N. Strafford, *J. Less-Common Met.* **37**, 299 (1974).
5. A. Menzies and K. N. Strafford, *Corros. Sci.* **15**, 69 (1975).
6. A. Menzies and K. N. Strafford, *Corros. Sci.* **15**, 91 (1975).
7. A. L. Dowson, Ph.D. thesis, Newcastle upon Tyne Polytechnic, 1988.
8. I. A. Menzies and K. N. Strafford, *J. Less-Common Met.* **12**, 85 (1967).
9. A. E. Jenkins, *J. Inst. Met.* **84**, 1 (1955–1956).
10. S. Anitov and S. A. Gorbunov, *J. Appl. Chem. USSR* **34**, 703 (1961).
11. B. Champin, L. Graff, M. Armand, G. Beranger, and C. Coddet, *J. Less-Common Met.* **69**, 163 (1980).
12. A. Grossley, *Trans. Met. Soc. AIME* **245**, 1963 (1969).

13. A. M. Chaze and C. Coddet, *J. Less-Common Met.* **157**, 55 (1990).
14. I. A. Menzies and K. N. Strafford, Proc. 3rd Int. Congr. on Corrosion of Metals, Mir, Moscow, Vol. 4, p. 93.
15. G. Welsch and A. I. Kahveci, in *Oxidation of High-Temperature Intermetallics*, T. Grobstein and J. Doychak, eds. (TMS/AIME, 1988), p. 207.
16. G. H. Meier, D. Appalonia, R. A. Perkins, and K. T. Chiang, in *Oxidation of High-Temperature Intermetallics*, T. Grobstein and J. Doychak, eds. (TMS/AIME, 1988), p. 185.
17. Y. Umakoshi, M. Yamaguchi, T. Sakagami, and T. Yamane, *J. Mater. Sci.* **24**, 1599 (1989).
18. N. S. Choudhury, H. G. Graham, and J. W. Hinze, in *Properties of High Temperature Alloys with Emphasis on Environmental Effects*, Z. A. Foroulis and F. S. Pettit, eds. (The Electrochemical Society, Princeton, 1976), p. 668.
19. S. Becker, A. Rahmel, M. Schorr, and M. Schutze, *Oxid. Met.* **38**, 425 (1992).
20. J. B. McAndrew and H. D. Kessler, *Trans. AIME J. Met.* 1348 (1956).
21. R. A. Perkins, K. T. Chiang, G. H. Meir, and R. Miller, in *Oxidation of High-Temperature Intermetallics* (The Minerals, Metals and Materials Society, Warrendale, 1988), p. 157.
22. T. A. Wallance, R. K. Clark, K. E. Widemann, and S. N. Sankaran, *Oxid. Met.* **37**, 111 (1992).
23. H. L. Du, Ph.D. thesis, University of Northumbria at Newcastle, 1991.
24. P. K. Datta, K. N. Strafford, H. L. Du, D. B. Lewis, and J. S. Gray, in *Heat-Resistant Materials*, Proc. 1st Int. Conf., K. Natesan and D. J. Tillack, eds. (Fontana, Wisconsin, 1991), p. 323.
25. H. L. Du, P. K. Datta, J. S. Gray, and K. N. Strafford, *Oxid. Met.* **39**, 107 (1993).
26. H. L. Du, P. K. Datta, B. Lewis, and J. S. Burnell-Gray, *Corros. Sci.* **36**, 631 (1994).
27. A. Preece and G. Lucas, *J. Inst. Met.* **81**, 219 (1952).
28. J. Sartell and C. Li, *J. Inst. Met.* **90**, (1961–62).
29. C. Phalnikar, E. Evans, and W. Baldwin, *J. Electrochem. Soc.* **103**, 429 (1956).
30. G. Wood, I. Wright, and J. Ferguston, *Corros. Sci.* **5**, 645 (1965).
31. L. Czerski, S. Mrowec, and T. Werber, *J. Electrochem. Soc.* **109**, 273 (1962).
32. A. Brückman, *Corros. Sci.* **7**, 51 (1967).
33. K. N. Strafford and P. K. Datta, *Mater. Sci. Technol.* **5**, 765 (1989).
34. K. N. Strafford, P. K. Datta, A. F. Hampton, A. Starr, and W. Y. Chan, *Corros. Sci.* **29**, 775 (1989).
35. R. A. Perkins, in *Proc. Int. Conf. on the Behaviour of High Temperature Alloys in Aggressive Environments*, Petten (NH) The Netherlands, 1979, p. 617.
36. H. J. Grabke, R. Möller, and A. Schnaas, in *Proc. Int. Conf. on the Behaviour of High Temperature Alloys in Aggressive Environments*, Petten (NH) The Netherlands, 1979, p. 759.